RUNX1 FUNCTION IN MOUSE SKIN TUMOR FORMATION

Honors Thesis
Presented to the College of Agriculture and Life Sciences
Biology Department of Genetics and Development
of Cornell University
in Partial Fulfillment of the Requirements for the
Research Honors Program

By
Charlene S. Hoi
May 2010

Tudorita Tumbar

ABSTRACT

Adult stem cells, which are characterized by their slow-cycling, multi-potent and self-renewing nature, are crucial in maintaining tissue homeostasis and responding to wound-stimuli. In addition to these classical roles, one current hypothesis posits that deregulated adult stem cells may in fact be the origin of cancer-initiating cells. Within the epidermis, hair follicle stem cells (HFSCs) give rise to and maintain the hair follicle structure through a series of remodeling phases known as 'hair cycles'. The transcription factor Runx1, also known as AML1, plays a role in the activation of HFSCs by prolonging the quiescent phase of the hair cycle when ablated. Coincidently, Runx1 is also translocated in 20-30% of patients afflicted with the blood-related disease acute myeloid leukemia. In this study, we explore the role that Runx1 may have in skin tumorigenesis by using a mutagen (9,10-Dimethyl-1,2-benzanthracene, DMBA) and a phorbol ester mitogen (12-O-tetradecanoylphorbol-13-acetate, TPA) in a two-step, oncogenic protocol. First, we observe that epithelial-specific Runx1-mutant mice show decreased levels of phosphorylated Stat3 and acquire significantly fewer papillomas than their wild-type littermates in response to carcinogenic drug treatment, a phenotype which is reversed when the cell cycle regulator p21 is simultaneously knocked-out. Second, cells initially expressing Runx1 contribute to tumor formation. Lastly, induced removal of functional *Runx1*, which is up-regulated in tumors, following tumor formation actually resulted in a reduction in overall tumor volume. Taken all together, these results suggest that *Runx1* functions upstream of p21 and is involved in not only the initiation of tumors, but also their proliferation and progression, possibly via the Jak/Stat pathway.

INTRODUCTION

Epithelial stem cells exist throughout the lifetime of the animal and are thought to be prime targets for mutagenic events which then generate the cancer stem cells (CSCs) responsible for skin tumor formation (Perez-Losada and Balmain 2003). Of these, hair follicle stem cells (HFSCs) are most susceptible to tumor promotion, given their extremely slow-cycling nature and tendency of retaining carcinogens (Morris 2000). Other organ systems provide strong evidence for this CSC from primary stem cell (SC) model. In blood, AML tumor cells share the same cell-surface markers as normal hematopoietic stem cells (HSCs) (Bonnet and Dick 1997). In intestine, lineage tracing of Lgr5-expressing stem cells confirms contribution of these intestinal SC to cancer (Barker, Ridgway et al. 2009). Cells of the hair follicle (HF), including HFSCs, have already been identified in a variety of skin cancers (Stenbach 1980; Morris 2000; Owens and Watt 2003), including malignant human basal cell carcinoma (Hutchin, Kariapper et al. 2005; Massoumi, Podda et al. 2006; Lorz, Segrelles et al. 2009) and mouse squamous cell carcinomas (Faurschou, Haedersdal et al. 2007).

Runx1/AML1 is part of a family of three transcription factors (TFs), all of which are involved in cancer (Blyth, Cameron et al. 2005), tissue stem cell regulation (Appleford and Woollard 2009) and development (Coffman 2003). Up until now, examination of Runx1 has primarily been in the hematopoietic system. Germ-line Runx1 knockouts are embryonic lethals due to the requirement for Runx1 during early HSC emergence (Speck and Gilliland 2002; Taniuchi, Osato et al. 2002), though Runx1 is dispensable during later adult homeostasis (Taniuchi, Osato et al. 2002; Ichikawa, Asai et al. 2004; Growney, Shigematsu et al. 2005). Additionally, 20-30% of patients with acute myeloid leukemia (AML) have a translocation of the Runx1 gene (Speck and Gilliland 2002; Blyth, Cameron et al. 2005; Mikhail, Sinha et al. 2006). Although Runx1 involvement in the epidermis has yet to be fully characterized, its function has been explored, particularly the hair follicle (HF) (Raveh, Cohen et al. 2006; Osorio, Lee et al. 2008).

The HF is an appendage of the epidermis that extends into the underlying dermis (Schneider, Schmidt-Ullrich et al. 2009). It is maintained by a specialized population of SC that

have the ability to self-renew and differentiate for extended periods of time. These so called HFSCs regulate HF progression through cycling stages of quiescence (telogen), growth and proliferation (anagen) and regression (catagen) (Figure 1A). As this dynamic micro-organ cycles, old hair shafts are shed from the skin during a process termed exogen (Muller-Rover, Handjiski et al. 2001). During tissue homeostasis, HFSCs reside in a region known as the bulge (Schneider, Schmidt-Ullrich et al. 2009). HFSCs were first discovered by their slow-cycling and label-retaining properties (Cotsarelis, Sun et al. 1990; Tumbar, Guasch et al. 2004; Schneider, Schmidt-Ullrich et al. 2009). In mouse, bulge stem cells express molecular markers including, though not limited to, CD34 (Trempus, Morris et al. 2003), high levels Keratin-15 (Liu, Lyle et al. 2003), and a gamut of markers shared by other adult SC compartments such as nestin (Hoffman 2007) and Lgr5 (Jaks, Barker et al. 2008). Additionally, *Runx1* has been shown to be dynamically expressed in the HF throughout the different stages of the hair cycle.

In telogen, *Runx1* is found in the bulge as well as the hair germ, which is a small epithelial structure beneath the bulge apparent. In anagen, *Runx1* is expressed in the outer root sheath of the hair follicle as well as in transit amplifying matrix cells later during the stage. In catagen, *Runx1* is expressed in the epithelial strand of the regressing hair shaft (Raveh, Cohen et

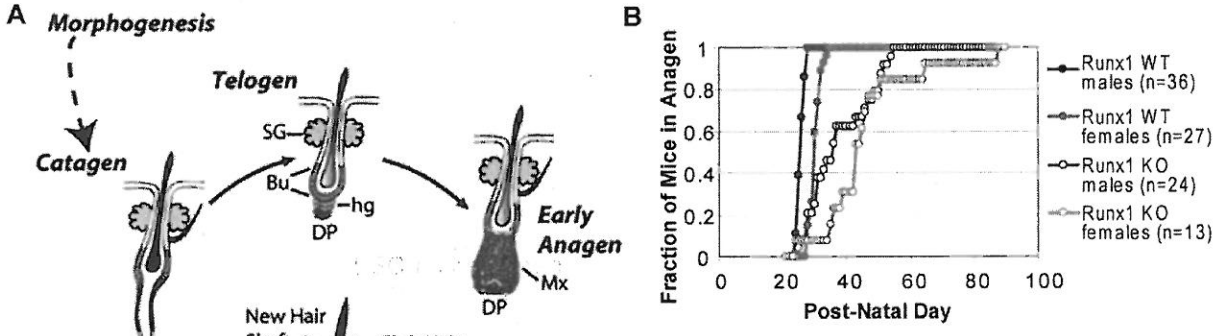

Figure 1 (A) Schematic showing the hair cycle and its three phases: telogen (quiescent phase), anagen (proliferative phase), and catagen (regressive phase), which repeat in this order throughout the animal's lifetime (image adapted from (Zhang, Cheong et al. 2009) (B) Characterization of when WT and cKO mice enter anagen. In WT mice, the first hair cycle is synchronous, beginning with telogen at ~PD20, followed by two weeks of anagen at ~PD24 for males and ~PD27 for females (solid circles). Runx1 cKO mice, however, have a perturbed cycling pattern for their first anagen, being delayed in their telogen-anagen transition for up to 6 weeks (empty circles).

al. 2006; Osorio, Lee et al. 2008). Due to its role in HSC emergence, Runx1 function in skin is studied via a conditional Runx1 knockout (cKO). Constitutive keratin-specific inactivation of *Runx1* by removal of the Runt homeo-domain important in DNA-binding and functionality perturbs normal homeostasis, as evidenced by the prolonged transition from telogen to anagen that we observed (Figure 1B). Absence of functional Runx1 resulted in a severe defect of HFSC activation (Raveh, Cohen et al. 2006; Osorio, Lee et al. 2008) as well as up-regulation of an important cell cycle regulator, p21 (Osorio, Lee et al. 2008).

p21 is a well-established cell cycle inhibitor, mediating cell exit from quiescence (G0) and reentry to the cell cycle. It is also a known tumor suppressor gene, sensitizing mice deficient for p21 to tumor formation (Topley, Okuyama et al. 1999) and working primarily via *ras*-mediated tumorigenesis (Oskarsson, Essers et al. 2006; Missero, Di Cunto et al. 2008). Given the altered p21 levels in Runx1 cKO mice, it is possible that a genetic interaction exists between the two. This in turn leads to the interesting question of whether Runx1 functions in skin tumor formation and if it does so via interaction with p21.

To address Runx1 in skin tumorigenesis, we treated mice with two carcinogens: DMBA (to mutate the H-ras oncogene) and TPA (to induce proliferation) (Hennings, Glick et al. 1993) while also making use of lineage tracing techniques and inducible Runx1 cKO mice. To delineate Runx1's putative interaction with p21, we generated and analyzed tumorigenesis in double-KO mice. The implications of this study are two-fold. First, our system allows for advancement in understanding the function of adult stem cells in cancer formation. Second, we begin to address the relevance of a possible target for gene therapy during different stages of cancer. We hypothesize that Runx1's apparent role in HFSC activation will translate into an equally important role for this TF during skin tumor formation, be it at one of the relevant stages of carcinogenesis: initiation, promotion, progression to malignancy, or any combination of these.

MATERIALS AND METHODS

Generation of mice

Conditional Runx1 epithelial-specific knockout (cKO) mice as well as their wild-type (WT) and heterozygous (Het) littermates were generated by first mating K14-Cre;$Runx1^{+/+}$ mice (CD1) with $Runx1^{fl/fl}$ mice (C57Bl6) (Vasioukhin, Degenstein, et al. 1999; Growney, Shigematsu et al. 2005) to generate a hemizygous F1 with the genotype K14-Cre;$Runx1^{fl/+}$. These F1 were then again crossed with $Runx1^{fl/fl}$ mice to generate experimental mice. Any mouse negative for K14-Cre, therefore containing intact Runx1 alleles are referred to as wild type (WT: this included the floxed, un-excised Runx1 allele) while K14-Cre^{+};$Runx1^{fl/+}$ were referred to as heterozygous (Het) and K14-Cre^{+};$Runx1^{fl/fl}$ as knockouts (cKO).

Inducible Runx1 KO (iKO) were generated in a similar manner, except instead of K14-Cre mice, they were _-actin-CreER (C57Bl6). To ensure that all experimental mice are homozygous for the floxed Runx1 allele, _-actin-CreER;$Runx1^{fl/fl}$ from the F2 were crossed once more with $Runx1^{fl/fl}$ before being used for the experimental mating.

For lineage tracing of Runx1-expressing cells, we used Runx1-CreER (C57Bl6) mice containing the Cre-recombinase inserted in the Runx1 endogenous locus downstream of the Runx1 promoter, combined with a Rosa26 line of mouse containing the LacZ reporter. Genotyping of Cre-ER mice was performed as previously described (Hayashi and McMahon 2002).

Double Runx1/p21 knockouts (Runx1 cKO;p21 KO), single Runx1 or p21 knockouts (Runx1 cKO;p21 WT and Runx1 WT;p21 KO, respectively) and wild-type mice (Runx1 WT;p21 WT) were generated by first mating $Runx1^{fl/fl}$ mice with $p21^{-/-}$ mice (Jackson Laboratories strain B6;129S2-*Cdkn1atm1Tyj*/J) to generate $Runx1^{fl/+}$;$p21^{+/-}$. These F1 were then self-crossed to generate homozygous $Runx1^{fl/fl}$ that are either $p21^{+/+}$ or $^{-/-}$. Meanwhile, K14-Cre^{+};$Runx1^{fl/+}$ mice were also crossed with $p21^{-/-}$ to obtain K14-Cre^{+};$Runx1^{fl/+}$;$p21^{+/-}$. These F1 were then crossed again to either $p21^{+/+}$ or $p21^{-/-}$ to obtain K14-Cre^{+};$Runx1^{fl/+}$ mice that are either p21 WT or KO. In the final step, K14-Cre^{+};$Runx1^{fl/+}$;p21 mice are crossed with $Runx1^{fl/fl}$;p21 mice in such a way that

would generate either p21 WT (both parents p21 WT) or p21 KO (both parents p21 KO), with a mix of Runx1 WT, Het, or cKO.

All genotypes were asserted via polymerase chain reaction (PCR) and the appropriate primer pairs. In this study, black C57Bl6 and brown CD1/SV129 mice are used, which conveniently provides a gauge for hair cycle stage by virtue of melanocyte recruitment during anagen phases only (Muller-Rover, Handjiski et al. 2001). While telogen and catagen are marked by lack of melanocytes, giving the skin a pink to white color, anagen is characterized by being gray and/or black.

Skin tumorigenesis

We generated papillomas through a two-step tumorigenic protocol which employs 9,10-Dimethyl-1,2-benzanthracene (DMBA) and 12-O-tetradeanoylphorbol-13-acetate (TPA). Although generally benign, these papillomas do sometimes progress into malignant squamous cell carcinomas (SCCs) (Hennings, Glick et al. 1993). We first shaved the hair off the back of the mice to expose the back skin. After applying 32ug DMBA dissolved in acetone, we waited one week to allow for targeted point mutation of codon 61 in the H-ras proto-oncogene to occur (Ward, Rehm et al. 1986). Following that week, the mice were thereby treated twice weekly with 12.4ug TPA, again dissolved in acetone, for up to 20 weeks. TPA serves as a mitogen in that it targets protein kinase C activity to induce proliferation.

Throughout this process, mice were shaved as necessary (as to allow full exposure of skin to the TPA) and the skin was monitored for both hair cycle (as indicated by skin color) and tumor formation on a weekly basis. Following these treatments, mice were aged for up to 14 more months to monitor the rate of conversion to SCCs. Malignancy was grossly characterized as physical changes in the tumor involving sudden sinking/down growth, vascularization, attachment to the fascia, and/or sudden increase in growth rate. Malignant conversions of tumors displaying any of the aforementioned qualities were confirmed via histological assessment of the tumor's morphology and of metastatic events by a trained veterinary pathologist (Dr. Rachel Peters).

Additional mice were also treated such that tumor and skin samples could be collected throughout the DMBA/TPA treatment period (at 8, 15 and 20 weeks) as well as afterwards.

Samples were then analyzed either by immunofluorescence staining or hematoxylin and eosin staining.

5-bromo-3-deoxy-uridine (BrdU) labeling

5-Bromo-3-deoxyuridine dissolved in phosphate buffered solution (PBS) was injected either subcutaneously (subQ) or intra-peritoneally (IP) at 25ug BrdU/g body weight. To generate label retaining cells (LRCs), mice were injected subQ six times during postnatal days (PD) 3, 4 and 5. LRCs were then chased for either three weeks (PD21) or five weeks (PD35). To label proliferative cells, a short-term BrdU pulse was administered via 2 IP injections spaced 6 hours apart. Mice were sacrificed 2 hours after the last injection, at which point skin samples were collected then further analyzed.

Tamoxifen-induced Cre-recombinase expression

In mice containing Cre-recombinase downstream of certain promoters (_-actin-CreER and Runx1-CreER), we used tamoxifen (TM) to bring the ER-sensitive Cre-recombinase enzyme to the nucleus. There, the enzyme then carries out the appropriate recombination events. For _-actin-CreER;Runx1$^{fl/fl}$, TM induction leads to excision of the fourth exon of Runx1 containing the Runt homeo-domain. For Runx1-CreER;Rosa26floxed mice, TM induction causes Runx1-expressing cells to be labeled by LacZ expression. TM was injected IP at 225mg TM/g body weight for two consecutive days.

Histology, immunofluorescence and X-gal analysis

Tissue samples were analyzed in a variety of ways. Fresh tissue (skin and/or tumors) was embedded in optimal cutting compound (OCT) for sectioning. 10_m sections were cut either serially or at 50-80_m intervals for staining.

Hematoxylin and eosin (HE) staining were used on both skin and tumor tissue. In skin, HE staining was used to confirm that a cKO not displaying any apparent tumors likewise did not show anomalies in the skin suggestive of neoplastic growth. In tumors, it was used to histologically confirm the status of SCCs versus non-malignant papillomas. Sections were fixed in 4% paraformaldehyde prior to successive incubations with hematoxylin and eosin, respectively, and finally sealed with basic 90% glycerol.

Immunofluorescence (IF) staining was used to analyze BrdU incorporation and cell marker expression throughout tumorigenesis. This involved keratins (K) 1, 5 and 15, CD-34, _6-integrin, E-cadherin and loricrin. Finally, Runx1 and phosphorylated Stat3 (pStat3) were also analyzed for qualitative levels throughout tumorigenesis. 10_m sections were first fixed in 4% paraformaldehyde. They were then incubated with the appropriate primary antibodies from: (1) rat anti [_6-integrin and CD-34 (both 1:150, BD Pharmingen), BrdU (1:300, Abcam, also an extra HCl wash prior to incubation), E-cadherin (1:500, Sigma)], (2) rabbit anti [K1 (1:500, Covance), Loricrin (1:200, E. Fuchs, Rockefeller University), Runx1 (1:8000, T. Jessell, Columbia University), pStat3 (1:50, Cell Signaling) (3) guinea pig anti [K5 and K15 (1:5000, E. Fuchs, Rockefeller University)]. Nuclei were labeled by Hoechst. All secondary incubations were at 1:500 (except BrdU, which was at 1:300).

X-gal staining either in thin sections or whole skin was used to analyze _-galactosidase activity from the LacZ gene. For thin sections, 10_m sections were first fixed in 0.1% gluteraldehyde then incubated with X-gal solution at 37°C for 18-24 hours. Sometimes a cross stain with hematoxylin was done to bring contrast to the tissue. Whole mount staining was done to grossly and quickly assess LacZ activity. Entire back skin containing tumors was collected and washed in PBS to separate dermis and adipose tissue from the epidermis. Following this, tissue was fixed in 2% periodate-lysine paraformaldehyde (McLean and Nakane 1974) and then incubated with X-gal solution at 4°C for 36-48 hours (Kopan, Lee et al. 2002)

All images were acquired using a light fluorescent microscope (Nikon) and IP-Lab software. Brightness, contrast and level adjustments were then made using Adobe Photoshop and/or Adobe Illustrator.

Statistical Analysis

Data shown are averages and standard deviations. Significance and p-values were calculated using one and two-tailed Student T-tests.

RESULTS

Runx1 cKO acquire fewer tumors than WTs and have lower pStat3 levels

To address whether Runx1 is important in skin tumor formation, we used a total of 28 WT and 24 Runx1 cKO mice treated with DMBA and TPA for up to twenty weeks (Figure 2A, 40% of the treatments were done by Caroline Piskun). Since Runx1 loss perturbs hair cycle timing, in order to obviate any variation that might be introduced by hair stage during DMBA induction on ultimate tumor formation (Mukhtar 1995), we induced mice at three different time points: initiation in their first telogen (PD21 for WT and PD28 for cKO), in their first anagen (PD28 for WT and PD33-81 for cKO), and finally in their second telogen (PD55-115 for both WT and cKO) Furthermore, the second telogen of mice is long enough that littermate WT and cKO mice could be induced at the same age, even considering the delay in HF cycle in cKO mice.

Throughout the treatments, skin color changes, which are indicative of hair cycle stage, as well as tumor formation were recorded. By the end of the treatment period, Runx1 cKO mice had a significantly longer latency in tumor formation and were half as likely to develop tumors (Figure 2C, left panel). In addition, of those mice that did form tumors, the number of tumors acquired was significantly decreased (Figure 2B, C right panel and E). While the number of hair cycles that HF underwent during the period of treatment did correlate positively with the number of tumors that formed (Figure 2D), it was apparent in the 2^{nd} telogen group of mice, in which WT and cKO HFs underwent the same number of hair cycles, that genotypic difference has a determining role in skin tumorigenesis.

To ensure that small papillomas were not missed during tumor counts, serial sections were made of a 20 week cKO mouse that did not display any apparent tumors. HE staining showed no small anomalies or lesions in the skin that might represent budding tumors that failed to progress to sizable papillomas. cKO mice were therefore failing to form tumors altogether.

The reduced tumor incidence of Runx1 cKO suggests that Runx1 may be working as a proto-oncogene in skin. Previous studies have shown that the absence of proto-oncogenes might actually accelerate the rate of malignant transformation (Greenhalgh and Yuspa 1988), so we next looked at the progression rate of malignant squamous cell carcinomas (SCCs). The

DMBA/TPA protocol employed in these experiments has been reported to generate benign papillomas which convert to malignancy at a rate of about 15% in the C57/Bl6 mouse strain and 37.5% in the CD1 mouse strain (Hennings, Glick et al. 1993). Mice that were finished with their

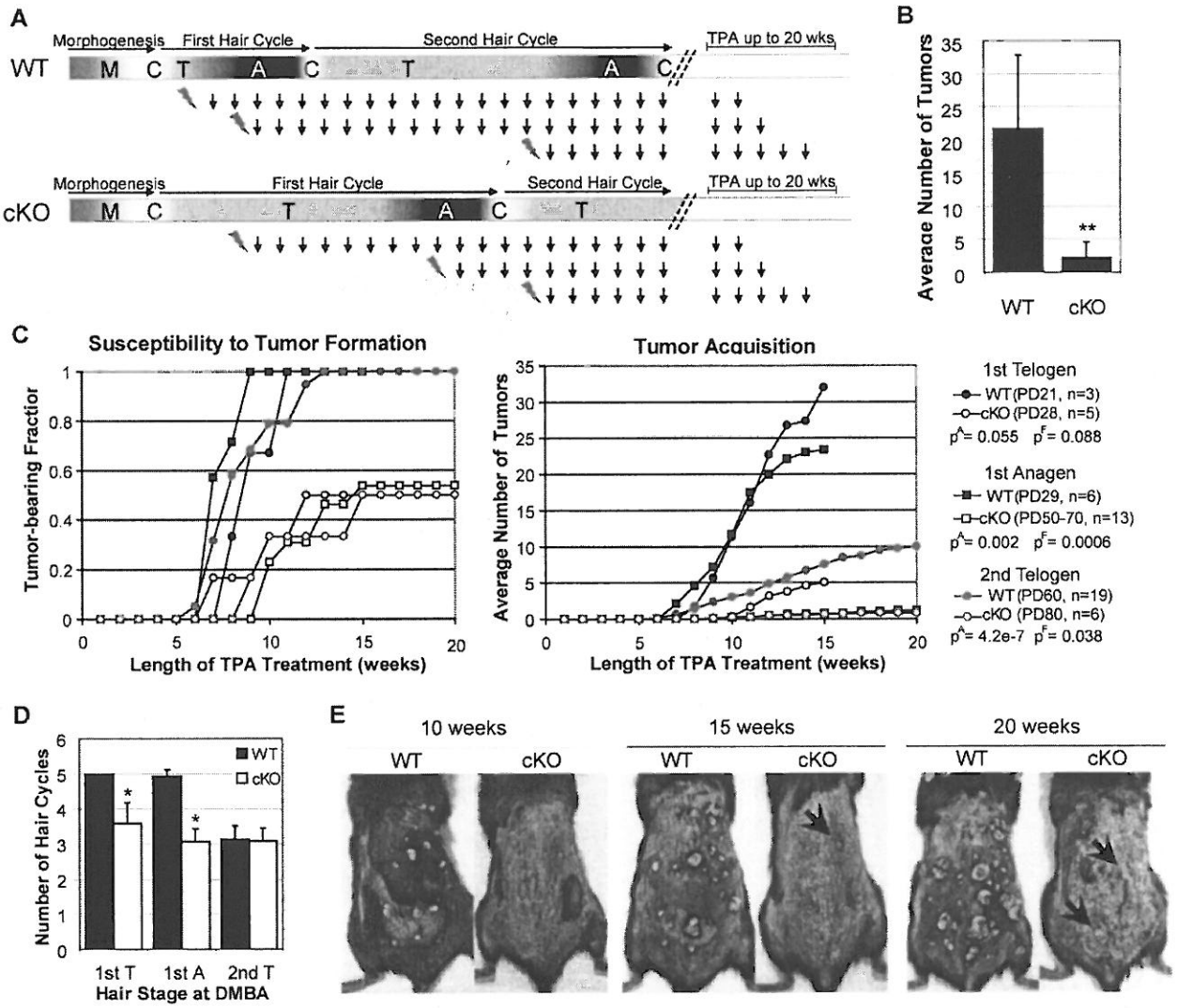

Figure 2 (A) Schematic of the induction scheme used for tumorigenesis in WT (top) and cKO (bottom) mice. First telogen induction was at PD21 for WT mice and at PD28 for cKO mice. First anagen induction was at PD28 for WT mice and anywhere between PD33 and PD81 for cKO mice (anagen onset gauged by skin color). Induction in the second telogen was consistent between littermates and ranged anywhere between PD60 to PD115. (B) Averaged tumor numbers of WT mice from all three stages versus cKO mice from all three stages (** indicates p-value <0.05). (C) Graphs showing tumor incidences, either occurrence (left or number (right), for the three different stages of both WT and cKO (p^F and p^A are p-values for formation and averages, respectively, between WT and cKO mice within the same induction group). (D) Average number of hair cycles experienced by a mouse in a given treatment group (* indicates p-value < 0.001). (E) Representative WT and cKO mice from the first telogen group showing differences in tumor incidence (cKO tumors indicated with black arrow). Note that tumor formation in the cKO mouse is slightly delayed and drastically decreased from that in the WT mouse.

TPA treatment were aged up to 14 additional months and monitored for malignant transformation. As mentioned in the methods, this process is typified as involving sudden sinking/down growth, vascularization, attachment to the fascia, and/or sudden increase in growth rate. When mice displayed any of these criteria, samples of tumors and internal organs were harvested for histological analysis. Tumors themselves were gauged histologically (Figure 3A and B) while organs were analyzed for signs of metastasis with help from Dr. Rachel Peters, a trained pathologist (Figure 3C).

Of the 28 WT and 24 cKO mice, 8 WT mice and 1 cKO mouse developed SCCs. Given the approximate 20% reduction in tumor number of cKO mice (Figure 2B), both conversion rates come out to be ~30%. Although the single incidence of an SCC in the cKO is not enough to assertively conclude that Runx1 cKO does not reduce the conversion rate of tumors, it is suggesting at the least that it is not accelerating it. Given the low rate of malignant conversion in this genetic background, further investigation into the conversion rate would require many more cKO mice to account for the decreased tumor incidence. Alternatively, one could transfer the mice onto a genetic background that is more susceptible to malignant transformations, such as FVB (Hennings, Glick et al. 1993)

To investigate why cKO mice were forming fewer tumors, we began by looking within tumors for differences in *Runx1* levels and/or other markers. As has been previously reported, *Runx1* was found at high levels in papillomas (Malanchi, Peinado et al. 2008). Interestingly enough, however, this occurred in similar distribution patterns in both WT (7/8, Figure 3D, E and F) as well as cKO (3/3, Figure 3D) papillomas. The presence of *Runx1* in cKO tumors suggests that tumors arising in the cKO might arise from regions of inefficient K14-Cre activity. Furthermore, the high levels of *Runx1* hint at a putative role for Runx1 within the tumors themselves.

Also of interest were cell surface markers such as _6-integrin, CD34, K1, K5, E-cadherin and loricrin. _6-integrin is specific to the basal layer while CD34 is bulge-specific (Trempus, Morris et al. 2003). K1 and K5 together mark the differentiated and undifferentiated layers of epithelia, respectively, and were used to characterize SCC progression by virtue of K1 loss

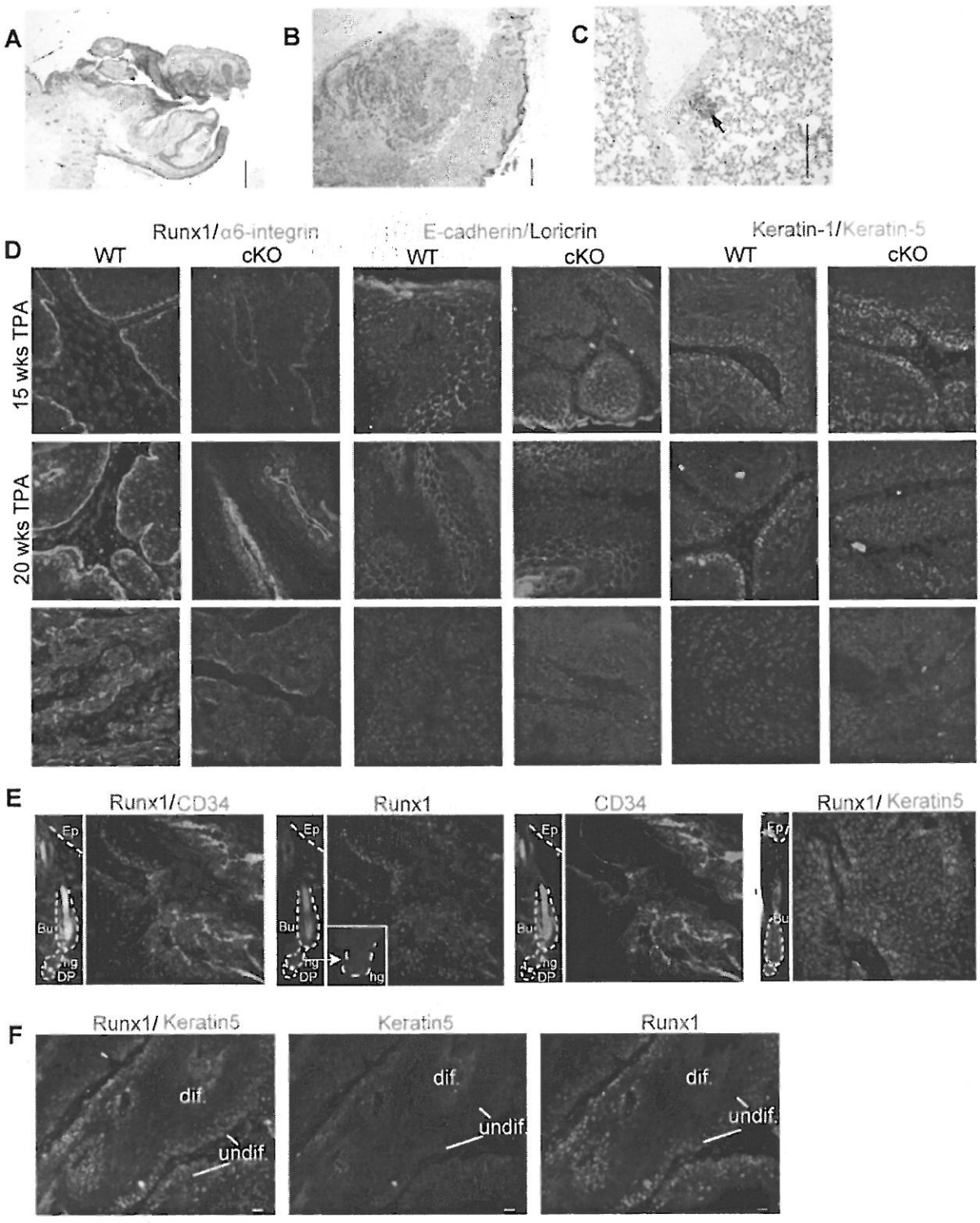

Figure 3 HE representations of (A) a papilloma (B) an SCC and (C) lung metastasis (black arrow) from the SCC in (B) (All indicated scale bars = 20um). Tumors at 15, 20, 3 months post TPA treatment and an SCC were analyzed for *Runx1* and also cell markers. (D) WT and cKO tumors at 15 weeks (top row) and 20 weeks (middle row) and WT and cKO SCC (bottom row) (Bu= bulge, Ep= epidermis, hg= hair germ, DP= dermal papillae). (E) WT tumor 3 months off treatment with accompanying panels showing normal distribution of CD34, *Runx1* and Keratin 5 in HF. Note that CD34 is bulge-specific. (F) Representative WT SCCs showing various degrees of differentiation correlating with K5 levels which co-localize with *Runx1*.

and K5 expansion (Figure 3D and F) (Roop, Krieg et al. 1988). E-cadherin is a component of adherens junctions in primarily epithelial compartments. As a player in cell-cell interactions, E-cadherin levels characteristically decrease during SCC progression of papillomas (Figure 3D) (Navarro 1991; Brouxhon 2007). A decrease in loricrin, a marker for the granular layer of the epidermis, also correlates with SCC progression (Figure 3D) (Abel, Angel et al. 2009). Since the papillomas detected in cKO mice appeared to express *Runx1* due to inefficient Cre-recombinase activity, it was not surprising that the distributions of all these markers were comparable in both WT and cKO papillomas both at 15 and 20 weeks (Figure 3D, CD34 not shown). Interestingly, *Runx1* expression co-localized with undifferentiated K5-expressing cells (Figure 3F) and _6-integrin, yet was not detectable in more differentiated K1-expressing cells. Finally, while 7 of 8 WT SCC expressed Runx1, the cKO SCC showed no Runx1 staining. Intriguingly, *Runx1* negative SCC (WT and KO) both had qualitatively higher levels and E-cadherin and lower levels of K5 (WT not shown, KO in Figure 3D), possible indications of a lesser progressed SCC than that which is analyzed in the other 7 WT. It is worth noting that the bulge specific marker CD34 is broadly expressed within tumors, and that observation previously attributed the possible origin of the tumors to CD34+ bulge cells (Trempus, Morris et al. 2007).

In addition to examining tumors, we also analyzed differences in marker expression between WT and cKO skin at early stages during the tumor formation process. This approach could potentially lead to a deeper understanding of why Runx1 cKO skin might be resistant to carcinogens. To that end, skin samples from regions devoid of tumors were collected at 8 weeks of TPA treatment (just prior to tumor formation), and also at 15 weeks (early papillomas) and 20 weeks (developed papillomas). We again looked at K1, K5, loricrin and E-cadherin, but also K15, which is expressed in the bulge as well as at low levels in the basal layer. To begin addressing possible molecular mechanisms for reduced tumorigenesis, we focused on a variety of proliferation-associated pathways including the EGF-receptor, Erk, PI3 kinase/Akt, and Jak/Stat. All have been implicated in cancer and tumorigenesis, given their role in gating proliferation.

While K5, K15, loricrin and E-cadherin patterns were comparable between WT and cKO (Figure 4A), K1 and phosphorylated Stat3 (pStat3) showed some variation (Figure 4A and B).

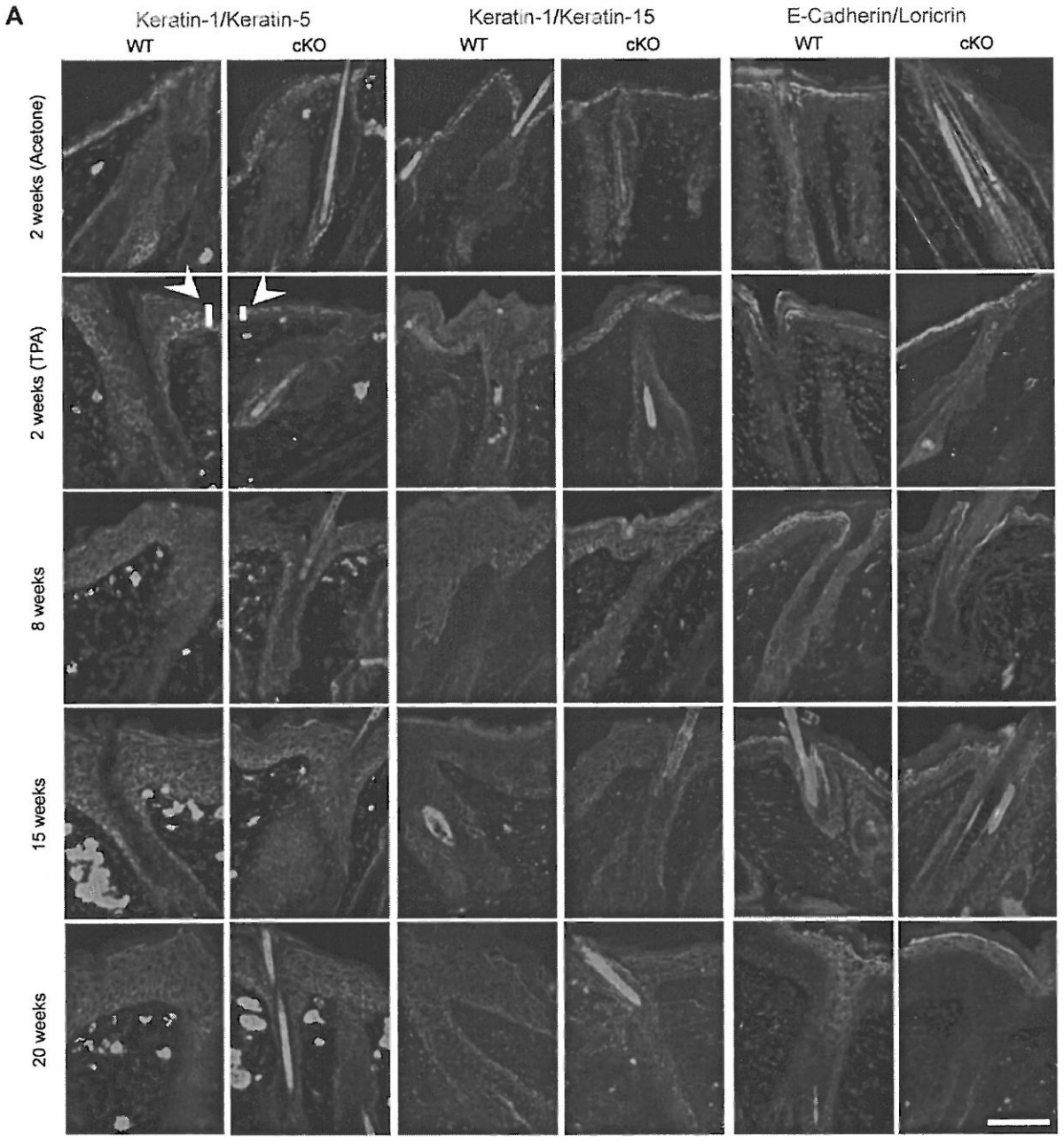

Figure 4 Skin sections throughout the treatment period were collected at 8, 15 and 20 weeks. Mice from the BrdU experiments were also used as representatives for short term response of skin to TPA treatment. (A) Epidermal hyper-proliferation was apparent in WT skin as early as 2 weeks after start of TPA treatment but not in cKO skin (arrows indicating bars that correlate with the amount of hyperproliferation). By 8 weeks and time points thereafter, cKO skin displayed similar epidermal expansion. (B) pStat3 was appreciably higher in WT skin than in cKO skin, as demonstrated in the 2 week skin samples shown. Scale bar= 75um.

pStat3 is a downstream effector of the Jak/Stat pathway, which is active during tumorigenesis (Valentino and Pierre 2006; Steelman, L. et al. 2008), primarily being involved with angiogenesis, tumor promotion and tumor progression (Park, Strock et al. 2003; Calvisi, Ladu et al. 2006). K1 staining of the differentiated epithelial layers emphasized the slight delay that cKO skin showed to epidermal hyperplasia at 2 weeks of TPA treatment (Figure 4a, indicated arrows). This difference was attenuated at later time points, but does demonstrate that, at least at early stages, Runx1 cKO skin seems resistant to the proliferative effects of TPA. pStat3 levels seemed to correlate with the degree of hyperplasia (data not shown), however comparisons between WT and cKO regions of comparable epidermal expansion showed convincingly that pStat3 was higher in the WT than in the cKO up through to 20 weeks of treatment. Reduced levels of pStat3 staining in cKO skin indicates reduced Jak/Stat signaling in cKO skin (Figure 4B), thereby providing a possible explanation for the reduced tumor formation observed in cKO animals. The difference was most apparent at the earlier stages, however was appreciable all throughout the treatment period (data not shown). Taken all together, Runx1 acts as a potential proto-oncogene in skin, possibly via the Jak/Stat pathway.

Runx1 mutant HFSCs are resistant to TPA-induced proliferation

Retardation in hyper-proliferation of cKO skin, as evidenced by K1 staining (Figure 4A) revealed a seeming resistance to TPA-induced proliferation. Given the fact that Runx1 cKO are known to be defective in HFSC activation, this observation can conceivably be a secondary effect of cKO HFSCs having a defect in proliferation. To see if HFSCs themselves are defective in proliferation even with TPA treatment, we quantified differences in proliferation using BrdU labeling assays.

HFSCs are slow-cycling in nature and therefore also known to be 'label-retaining'. If labeled during morphogenesis, HFSCs will retain that label until it is diluted via division. The first experiment gauged HFSC proliferation by the number of these label retaining cells (LRCs) before and after TPA treatment in WT and cKO mice (Figure 5A, 30% of the mice were generated by Caroline Piskun).

Following TPA treatment, WT demonstrated overall greater proliferation. Not only were fewer bulges labeled, but there were also fewer LRCs (Figure 5B, after TPA columns, and C). Conversely, Runx1 cKO possessed comparatively more labeled bulges and a greater number of LRCs, indicative of decreased levels of proliferation. After 2 weeks of TPA treatment, mice were often at different stages. Some cKOs seemed to possess a particularly strong phenotype and were still in telogen or early anagen by the end of the TPA treatment period. Since hair stage impinges on the number of LRCs (less in anagen than in telogen), a complimentary experiment was done in which mice were treated with TPA up until anagen onset, at which point proliferating cells were labeled with two BrdU injections spaced 6 hours apart. Since for WT mice, this meant only one or two treatments of TPA, all mice had half their backs treated with TPA and the other with acetone, separated by a silicon-based hydrophobic barrier. This technique allowed us to see whether TPA might have a different effect on WT versus cKO skin.

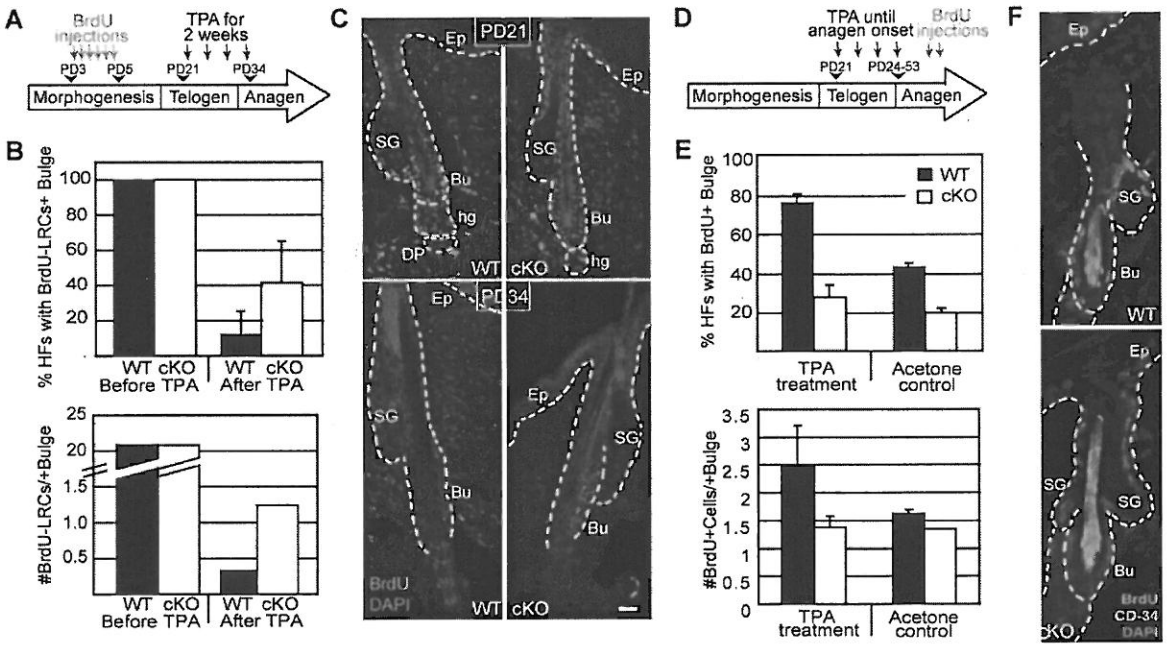

Figure 5 (A) Schematic showing the generation of label retaining cells (LRCs). Young mice were injected with BrdU 12 hours apart for three days from PD3-5. Weanlings were then treated for two weeks with TPA (from PD21-34). (B) Differences in LRC number were quantified between WT and cKO. Follicles were first scored for whether or not they contained a label (top panel, n=3) then further analyzed for the exact number of cells (bottom panel, n=1) (C) Representative follicles of WT and cKO at PD21 (just prior to TPA treatments) and PD34 (last day of TPA treatments). (D) Schematic of a complementary experiment in which short-term proliferating cells were labeled during the telogen-anagen transition. (E) Differences in label-incorporation were again quantified (n=3 for both groups). (F) Representative bulges of HF that are at anagen IIIB. Scale bar= 75um. (SG= sebaceous gland)

As expected, there were more proliferating bulges in WT skin than in cKO skin, a difference which was augmented in the presence of TPA (Figure 5E, top panel). Within positively labeled bulge compartments, the number of proliferating cells was significantly higher in WT skin than in the KO under TPA treatment only (Figure 5E, bottom panel and F). BrdU incorporation into acetone-treated skin revealed that KO HFs have a lower baseline level of bulges undergoing proliferation. The actual number of cells within a proliferating bulge compartment, however, is comparable. These differences then are amplified under TPA treatment In summary, BrdU analysis of HFSCs elucidates a defect in their proliferation despite treatment with TPA.

Runx1-expressing cells contribute to tumor formation

We next asked whether Runx1-expressing cells were possibly the cells of origin for tumor formation. To do this, we used Runx1-CreER mice crossed with Rosa26floxed mice which allow for lineage tracing of Runx1-expressing cells. The Rosa26floxed reporter mouse contains the LacZ gene downstream of a floxed stop codon such that upon Cre-recombinase activity, LacZ would be transcribed to produce _-galactosidase. Using this system, we induced labeling of Runx1-expressing cells via Runx1-driven CreER-recombinase expression and tamoxifen injection in mice just prior to tumor induction (Figure 6A, 50% of the mice were treated and analyzed by Cornelia Scheitz). As negative controls, Cre-negative mice induced with TM and Cre-positive induced with oil only were also analyzed. Following tumor formation, we then gauged _-galactosidase activity via LacZ staining.

The labeling efficiency of this schematic (optimized by David McDermitt) was at least 17% of bulge cells across all bulge cells in all follicles (data not shown). This calculation assumed that all bulge cells express Runx1 and that labeling of all bulge cells would be the maximum possible labeling. Although Runx1 is expressed in the bulge and the germ in telogen (Raveh, Cohen et al. 2006; Osorio, Lee et al. 2008), most of the labeling (>90%) was specific to the bulge due to an un-explained bias of the Cre against the cells of the hair germ (Figure 6B).

Three patterns of lineage traced tumors were found: fully labeled tumors, tumors with specks of labeled cells, and completely unlabeled tumors (Figure 6C). Of the 65 tumors from 8 different mice analyzed, two were fully labeled (Figure 6C, top left panel) while 3 were

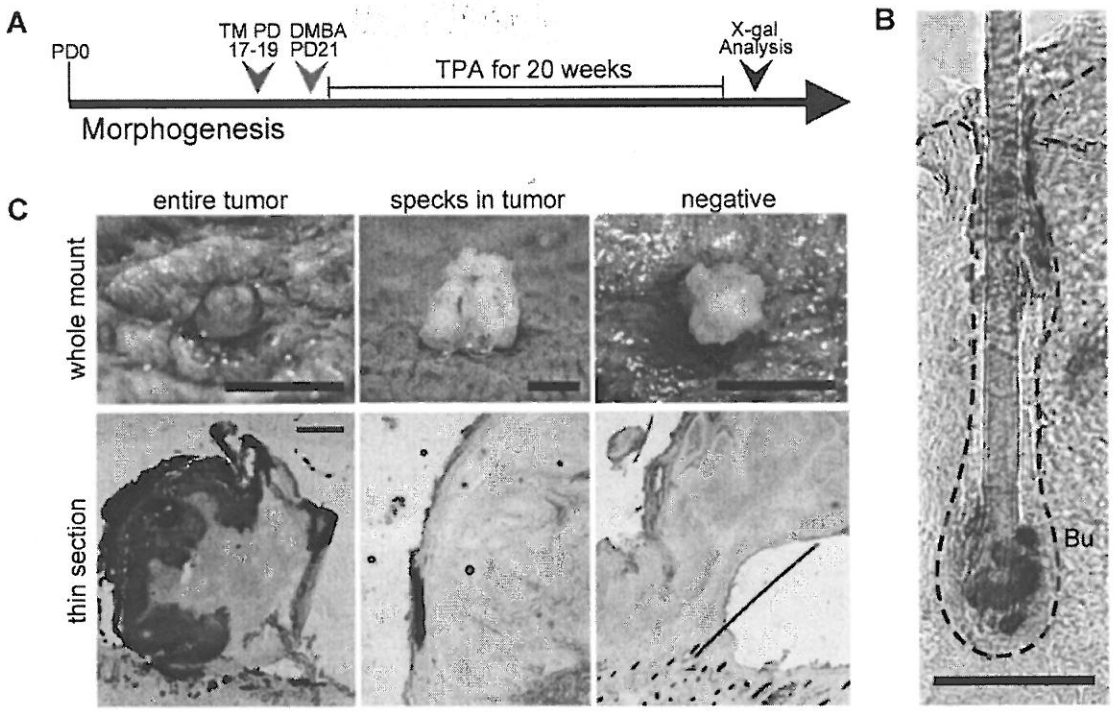

Figure 6 (A) Schematic of lineage tracing in tumors. Prior to DMBA and TPA induction and promotion of papillomas, Runx1-expressing cells were first labeled by injecting TM for two or three days over PD17-19. (B) Representative follicle pulsed with TM PD17-18 and chased for 3 days (scale bar= 50um). At the end of DMBA/TPA treatment, whole skin was collected and stained with the whole mount protocol, as described. (C) Three patterns of staining were found in the whole mount staining: tumors either entirely blue or entirely lacking in staining (first and third columns, respectively) or tumors with speckles (middle column). To check the penetration of the whole mount stain, further X-gal stain was performed on thin sections (scale bar whole mount, top row= 0.5cm, thin section, bottom row= 200um).

---

partially labeled with apparent blue speckles (Figure 6C, top middle panel). This made up 2.2% and 4.3%, respectively, leaving ~93.5% tumors unlabeled. Given the low efficiency of labeling to begin with, together with the fact that the mutagenesis procedure itself is random, this seemingly low fraction of labeled tumors in fact suggests a rather significant fraction of tumors originating from Runx1 expressing cells.

To ensure that the whole mount X-gal staining was not inefficient or restricted in its penetration of whole tissue, OCT samples were also made after the whole mount staining and sectioned so that thin section X-gal staining could be performed. All of the thin section stainings were in agreement with the whole mount staining (Figure 6C. bottom row). Negative controls of both the whole mount tissue and thin section showed no X-gal stainings (data not shown). The results from this lineage tracing demonstrate that Runx1-expressing cells do contribute to tumor

formation. Although a higher labeling efficiency would help to elucidate whether this contribution is preferential or not, our results indicate in the least that Runx1-expressing cells have the capacity to give rise to tumors

Runx1 is important in tumor maintenance

Next, we addressed the necessity for *Runx1* in tumor maintenance and possibly tumor progression to malignancy. To do this, I induced Runx1 inactivation with two successive injections of TM after tumor formation in _-actin-CreER;Runx1$^{fl/fl}$ mice (Figure 7A, B). _-actin is ubiquitously expressed and therefore serves as a reliable and efficient promoter for CreER-recombinase expression. Tumors of iKO and oil-control mice were measured every-other week following Cre induction to assess any changes in tumor volume. These changes were documented per tumor per mouse then averaged.

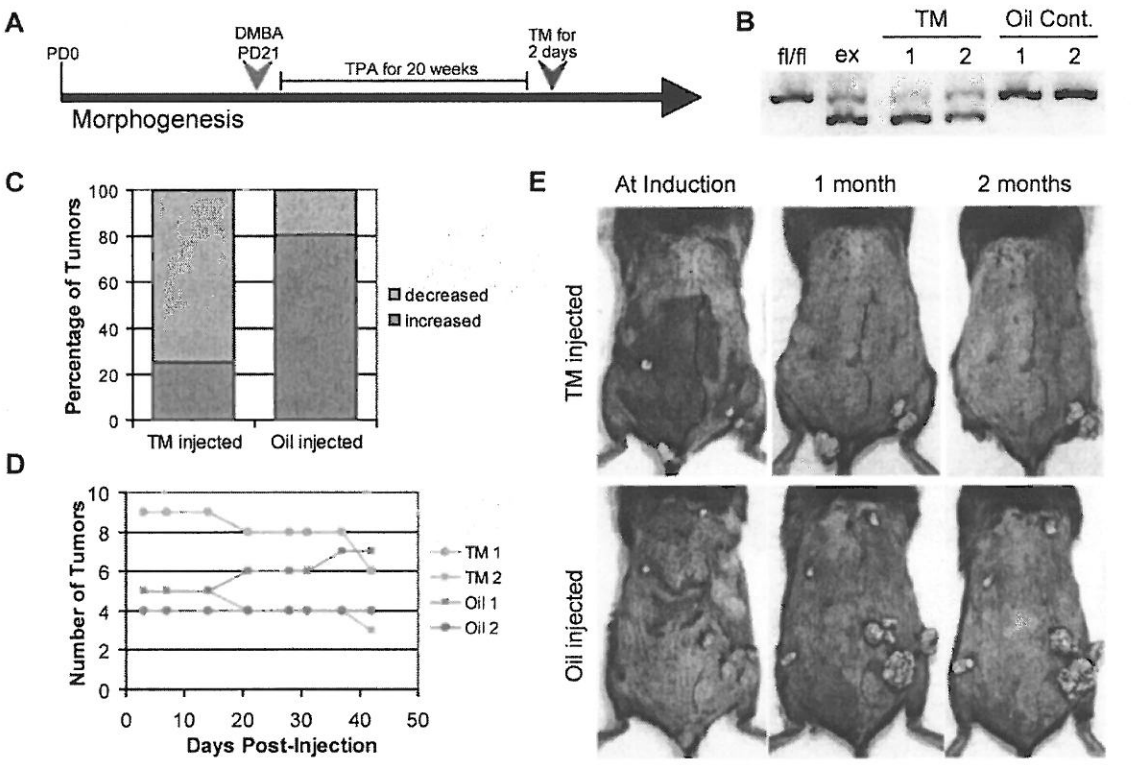

Figure 7 (A) Schematic showing induction of Runx1 removal. Following tumor induction in _-actin-CreER;Runx1$^{fl/fl}$ mice (n=4), Runx1 removal was induced by TM injection for two days in two of the mice. The other two were injected with oil only as negative controls. (B) PCR confirming Runx1 excision in TM injected mice versus oil injected mice. After TM induction, tumor measurements were made to provide calculations of tumor volume. Changes in tumor volume (C) as well as sheer change in tumor number (D) were apparent. (E) Representative photograph depict loss of tumors in TM treated mouse (top row) while tumor number and size increases in oil injected control mice (bottom row).

The 2 iKO mice showed significant negative changes in overall average tumor volume as compared to oil-control littermates (Figure 7C) as well as apparent changes in tumor number (Figure 7D). Although individual tumors in the mice induced with TM might have increased in size (Figure 7E), average changes in tumor volume of the animal were significant (data not shown). These data are preliminary and require future substantiation, however they do implicate that Runx1 is involved in tumor growth and long-term maintenance after carcinogenic treatment. It would be interesting to see if progression to SCC is affected at all in iKO mice. Based on the promise of these results, further experiments are underway in which an efficient epithelial-inducible system will be used.

p21 is downstream of Runx1 in tumor formation

Runx1 cKO skin contains elevated levels of the cell-cycle regulator and tumor suppressor p21 (Figure 8A, qRT-PCR done by D. McDermitt). Given p21's role in mediating a cell's exit from quiescence, we wondered whether this up-regulation had any significance in the delayed telogen- anagen phenotype characteristic of Runx1 cKO; similarly, given its role as a tumor suppressor, we asked its significance in tumorigenesis. To address these questions, we generated double knockout mice (Figure 8B). It has been shown that different strains respond to DMBA/TPA differently (Hennings, Glick et al. 1993), thus we used a mating scheme which would also produce full wild-types (Runx1WT;p21WT) as well as single knockouts (Runx1cKO;p21WT and Runx1WT;p21KO) in addition to our double knockouts such that all were on a similar genetic background and as such could be appropriately compared with previously treated Runx1 WT and cKO mice.

When Runx1/p21 mice were analyzed for their hair cycle phenotype, Runx1cKO;p21WT displayed a delayed telogen-anagen transition as previously observed (Figure 8C, open squares). Interestingly, Runx1cKO;p21KO mice were found to have an extremely long first telogen (Figure 8C, open circles). This phenotype was surprising given that a p21 mutant should be more susceptible to exiting quiescence. This exacerbated delay in the telogen-anagen transition may conceivably result from compensation events occurring within the skin in response to the simultaneous loss of a both Runx1 and p21.

We next asked how Runx1/p21 mice would respond to tumorigenesis. Given the upregulation of p21 in cKO skin and the resistance of cKO mice to tumor formation, we wondered if ablation of p21 would revert the tumor formation phenotype. To that end, 8 Runx1WT;p21WT, 3 Runx1Het;p21WT, 4 Runx1cKO;p21WT, 11 Runx1WT;p21KO, 5 Runx1Het;p21KO and 6 Runx1cKO;p21KO were induced with DMBA in their second telogen (to normalize the number of hair cycles) and treated with TPA twice weekly for 20 weeks (Karin Lilja performed 70% of the treatments).

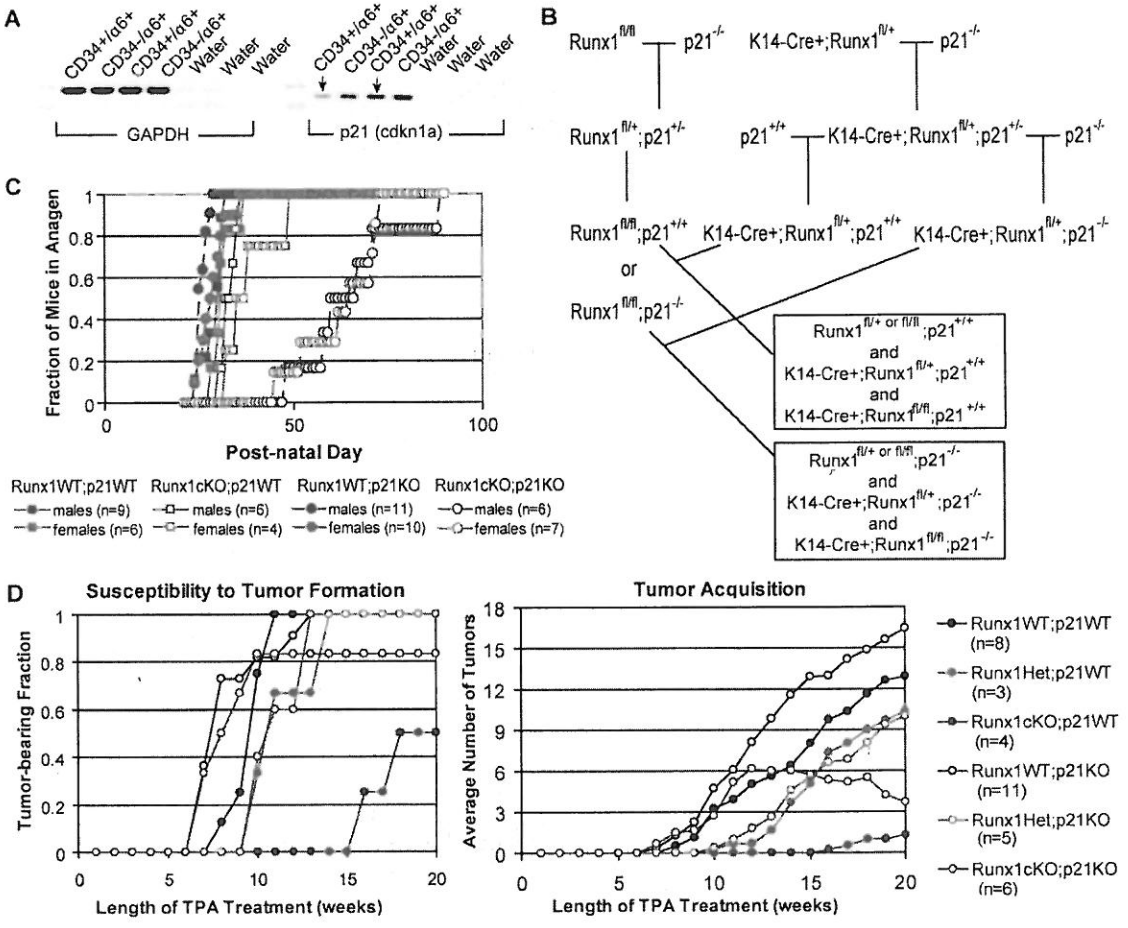

Figure 8 (A) qRT-PCR on FACS sorted bulge cells (CD34+, _6+) demonstrating elevated levels of p21 in Runx1 cKO skin as compared to WT mouse skin. To address the implications of this change, double knockout mice were made (B). Interestingly enough, the delayed anagen onset as previously reported (Osorio and Figure 1B) was exacerbated in the double knockout (C). Skin tumorigenesis in these mice reveal that Runx1 may lay upstream of p21, as suggested by the rescued tumor formation capabilities of double knockouts (D). The observed dip in tumor number following this rescued phenotype might be indicative of the importance of *Runx1* during tumor maintenance.

In p21 WT mice, Runx1 WT and cKO mice showed similar tumor formation trends as in CD1/C57Bl6 mice. All Runx1WT;p21WT mice developed tumors with a latency of ~8 weeks and average tumor count of ~12 (Figure 8D, solid black and blue circles). In Runx1WT;p21KO mice, tumor formation was accelerated, with a latency of ~6 weeks, and increased, with tumor numbers averaging 17 per mouse (Figure 8D, empty black circles). Intriguingly, Runx1cKO;p21KO mice showed some semblance to Runx1WT;p21KO tumorigenesis patterns. Tumor formation occurred in 80% of mice at slightly accelerated tumor latency. In tumor counts, the curve initially follows that in Runx1WT;p21KO mice, but then tapers off (Figure 8D, empty blue circles). Although the molecular mechanisms underlying the drop off in tumor numbers would require further investigation, these data provide some evidence for Runx1 being upstream of p21 in at least the pathway for skin tumorigenesis if not maintenance of homeostasis in HF.

DISCUSSION

Runx1/AML1, which has been shown to be absolutely necessary in HSC emergence, has proven to also have importance in HFSC homeostasis. Given the implications that translocation of Runx1 has in leukemia, we wondered if Runx1 would similarly have a role in skin tumor formation. In light of the prolonged quiescence that Runx1 cKO mice possess, we hypothesized and confirmed that Runx1 cKO do indeed form fewer tumors. To address the molecular mechanism underlying this tumor phenotype, we followed two strategies. First, we investigated the impact of Runx1 on the various stages of cancer (initiation, promotion and maintenance/progression). Second, we addressed the putative interactions between Runx1 and the cell cycle regulator and tumor suppressor p21, since p21 was up-regulation in Runx1 cKO bulge cells. We found that Runx1 cKO, which seems to function upstream of p21, acquire fewer tumors, possibly due to differences in involvement of the Jak/Stat pathway.

In our investigation of why Runx1 cKO acquire fewer tumors, we found a surprising up-regulation of *Runx1* even in tumors from cKO mice. Since Runx1 should have been inactivated in epithelial compartments (K14-promoter), inefficient Cre-activity might explain how some tumors were still able to form in cKO mice. Intriguingly, it has also been reported by us and others that TPA treatment leads to up-regulation of *Runx1* in the basal layer (BL) (Zhang, Biggs et al. 2004; Hoi, Lee et al. 2010). This detail warrants further investigation, for it may provide useful insight to the origin of these tumors which apparently have high levels of *Runx1*.

Runx1 acts as a potential proto-oncogene in mouse skin

Our study of Runx1 function in tumor formation can be broken down into the three stages of cancer development: initiation, promotion and maintenance/progression.

During the first stage of cancer, initiation, the initial transforming events/mutations take place. Although this could take on many avenues, including DNA repair mechanisms or apoptotic response to mutagens (Venkitaraman 2007; Jackson and Bartek 2009; Nakanishi, Niida et al. 2009), we chose to first assert whether or not Runx1-expressing cells contribute to actual tumor formation. It has been found that cells of the HF, including HFSCs, are the source of skin cancers (Morris 2000; Owens and Watt 2003), including human basal cell carcinoma (Massoumi, Podda

et al. 2006; Lorz, Segrelles et al. 2009) and mouse squamous cell carcinomas (Faurschou, Haedersdal et al. 2007) Since Runx1 is dynamically expressed in only certain compartments of the HF, one of which is the bulge, lineage tracing of these cells in tumor formation would provide further evidence for immediate HFSC contribution to skin tumorigenesis.

The DMBA/TPA carcinogenic protocol used generates papillomas which are clonal expansions of single cells mutated in *H*-ras (Kemp 2005). It therefore follows that the two fully labeled tumors we observed in our lineage tracing experiment were clonal expansions of Runx1-expressing cells which were likely mutated by the DMBA. The three cases in which tumors showed speckles of blue were not results of heterogeneous tumor cells, but rather seemed to be mere patches of skin that were labeled and then pushed up from the growing tumor mass below. These patches of blue skin may be from accidental wounds which the HFSCs then contributed to during healing (Taylor, Lehrer et al. 2000).

In light of the fact that TPA targets Runx1 levels in the BL (Hoi, Lee et al. 2010), one explanation for the prevalence of *Runx1* within tumors may be that tumors actually arise from the BL instead of HFSC. To address this question, it would be interesting to perform another lineage tracing of tumor formation in Runx1-CreER;Rosa26floxed mice, but with TM induction after TPA treatment to label Runx1-expressing cells within the BL.

Since our results indicate that tumors do arise from Runx1-expressing cells, the next step may be to study Runx1 function during initiation directly. It is possible that Runx1 cKO mice acquire fewer tumors because of a defect in this process (eg: elevated DNA-repair mechanisms or sensitized apoptotic response). Exploring this hypothesis would entail inducing Runx1 iKO immediately before DMBA application as well as at a time point soon after DMBA (at least 1 week should be allotted for mutagenesis to occur). This experiment would hopefully obviate any specious results that might occur as an artifact of Runx1 also affecting other key time points during tumor formation.

The next stage in tumor formation we assessed is proliferation, during which the transforming events cumulate and lead to hyper-proliferation which ultimately results in a tumor. TPA was used during our carcinogenic treatments to stimulate this very process, making it logical

that failure to respond to this process would affect tumor formation. We showed that mutant HFSCs fail to proliferate as readily as WT HFSC do; however, a defect in proliferation as the sole reason for decreased tumor formation would lead one to expect at least some lesions in KO skin resembling premature papillomas. Since none were found, mere defect in just proliferation may not be the reason for decreased tumor formation.

Although aberrant proliferation due to lack of Runx1 may be one explanation for reduced tumorigenesis, it is feasible that there are other factors involved. For one, an increase in apoptosis either initially during tumor initiation and/or later during tumor promotion could also result in decreased tumor formation. Analysis of these two processes via immunofluoresence staining of BrdU or Ki67 (for proliferation) and Caspase-3 (for apoptosis) in regressing tumors from iKO mice would be especially telling.

Runx1 effect on the tumor microenvironment

The final stage of tumor formation that we explored was tumor maintenance. Throughout tumor promotion, the tumor microenvironment (TME) becomes increasingly perturbed such that it can eventually sustain itself and even metastasize. The nature and development of the TME has become increasingly important in cancer biology (Demehri, Turkoz et al. 2009; Vidal, Salavaggione et al. 2010).

During our earlier investigation of why Runx1 cKO acquire fewer tumors, we found a decreased level of pStat3 in cKO skin during the early stages of tumor formation. The presence of pStat3 implicates involvement of the Jak/Stat pathway in skin tumorigenesis. This pathway, which is important in proliferation and angiogenesis (Park, Strock et al. 2003; Steelman, L. et al. 2008), has been shown to play a part in the tumor formation of other cancers, including the liver (Calvisi, Ladu et al. 2006) blood (Valentino and Pierre 2006). In fact, the prevalence of Stat3 of the STAT proteins in cancer has caused it to be identified as a putative target for cancer therapy (Yu, Pardoll et al. 2009). Although it remains to be seen whether the lower levels of pStat3 in Runx1 cKO skin is immediately responsible for the decreased tumor formation of Runx1 cKO mice, it is promising given the prevalence of the Jak/Stat pathway in tumorigenesis. In addition to proliferation and angiogenesis, the Jak/Stat pathway is also interacts with the cytokine IL6.

Cytokines are well established in the inflammatory response, a process which serves as a hallmark for perturbed TME (Wang and Dubois 2010). Given the decreased levels of pStat3 in Runx1 cKO skin, it is feasible that Runx1 may also have a role in remodeling of the TME.

While iKO reduction in tumor volume suggests a role for Runx1 in the maintenance of tumors, it would also be interesting to look at iKO generated at various stages during the carcinogenic protocol (perhaps 8 and 15 weeks). This would provide information on the importance of Runx1 on tumor promotion and TME development. Exploration of proliferation and/or apoptotic patterns in these alternative iKO tumors would help to further define the role that Runx1 may be having in tumor maintenance.

Runx1 interaction with p21 affects HFSC homeostasis and skin tumorigenesis

We showed that Runx1 and p21 interact genetically, with p21 laying downstream of Runx1. A chromatin immuno-precipitation (ChIP) would show directly whether *Runx1* physically binds to these promoters. Although we report that simultaneous KO of both Runx1 and p21 leads to an extreme delay in telogen-anagen onset, it has separately been shown *in vitro* that p21 KO actually rescues the proliferation defect of Runx1 cKO keratinocytes (Hoi, Lee et al. 2010), recapitulating the interaction that these two TF share.

The field of cancer biology is still developing, and it remains unknown whether adult stem cells are the primary source of cancer cells. From our studies, although we did not definitively show that HFSCs are the true origin of skin tumors, it is apparent that HFSC functionality does impinge on tumor formation. We demonstrated that Runx1 affects each stage of cancer development, and in fact may do so via the Jak/Stat pathway and also a downstream target, p21. Although we used a very refined system to study skin tumorigenesis, the implications of both the gene (Runx1) and the tissue (HF) are relevant in the advancement of studying adult stem cells in cancer formation. We have only just begun to delve into the molecular networks involved, yet already we see how involved adult stem cells homeostasis may be towards cancer.

ACKNOWLEDGMENTS

Much of this project would not have been possible without the help of many others. Caroline Piskun (Cornell c/o '08) contributed 40% of the tumorigenesis data and 30% of the LRC experiment data. Cornelia Scheitz (Cornell graduate student, 1st year) performed ~50% of the treatments on RunxCreER;Rosa26 mice and post-treatment analyses. David McDermitt (Lab technician) optimized the TM induction scheme for lineage tracing and calculated the labeling efficiency. He also produced the qRT-PCR in Figure 8A. Karin Lilja (Lab technician) did ~75% of the treatments on p21/Runx1 mice. Also thank you to Tudorita Tumbar and the rest of the entire Tumbar laboratory group for all the guidance, advice and support.

REFERENCES

Abel, E. L., J. M. Angel, et al. (2009). "Multi-stage chemical carcinogenesis in mouse skin: Fundamental and applications." Nature Protocols **4**(9): 1350-1362.

Appleford, P. J. and A. Woollard (2009). "RUNX genes find a niche in stem cell biology." J Cell Biochem **108**(1): 14-21.

Barker, N., R. A. Ridgway, et al. (2009). "Crypt stem cells as the cells-of-origin of intestinal cancer." Nature **457**: 608-611.

Blyth, K., E. R. Cameron, et al. (2005). "The RUNX genes: gain or loss of function in cancer." Nat Rev Cancer **5**(5): 376-387.

Bonnet, D. and J. E. Dick (1997). "Human acutemyeloid leukemia is organized as a hierarchy that originaes from a primitive hematopoietic cell." Nature Medicine(3): 730-737.

Brouxhon, S. (2007). "Sequential down-regulation of E-cadherin with squamous cell carcinoma progression: loss of E-cadherin via a prostaglandin E2-EP2 dependent posttranslational mechanism." Cancer Res(67): 7654-7664.

Calvisi, D., S. Ladu, et al. (2006). "Ubiquitous activation of *ras* and Jak/Stat pathway in Human HCC." Gastroenterology **130**(4): 1117-1128.

Coffman, J. A. (2003). "Runx transcription factors and the developmental balance between cell proliferation and differentitation." Cell Bio Int(27): 315-324.

Cotsarelis, G., T. T. Sun, et al. (1990). "Label-retaining cells reside in the bulge area of pilosebaceous unit: implications for follicular stem cells, hair cycle, and skin carcinogenesis." Cell **61**(7): 1329-1337.

Demehri, S., A. Turkoz, et al. (2009). "Epidermal Notch1 loss promotes skin tumorigenesis by impacting the stromal microenvironment." Cancer Cell **16**(1): 55-66.

Faurschou, A., M. Haedersdal, et al. (2007). "Squamous cell carcinoma induced by ultraviolet radiationoriginates from cells of thehair follicle in mice." Experimental Dermatology(16): 485-489.

Greenhalgh, D. A. and S. H. Yuspa (1988). "Malignant conversion of murin squamous papilloma cell lines by transfection with the fos oncogene." Mol Carcinogen **1**(2): 134-143.

Growney, J. D., H. Shigematsu, et al. (2005). "Loss of Runx1 perturbs adult hematopoiesis and is associated with a myeloproliferative phenotype." Blood **106**(2): 494-504.

Hayashi, S., and A. P. McMahon (2002). Efficient recombination in diverse tissues by a tamoxifen-inducible form of Cre: a tool for temporally regulated gene activation/inactivation in the mouse. Dev. Biol. 244:305–318.

Hennings, H., A. B. Glick, et al. (1993). "FVB/N mice: an inbred strain sensitive to the chemical induction of squamous cell carcinomas in the skin." Carcinogenesis(14): 2353-2358.

Hoffman, R. (2007). "The potential of nestin-expressing hair follicle stem cells in regenerative medicine." Expert Opin Biol Ther **7**(3): 289-291.

Hoi, C., S. E. Lee, et al. (2010). "Runx1 directly promotes proliferation of hair follicle stem cells and epithelial tumor formation in mouse skin." (in press) Mol Cell Biol.

Hutchin, M., M. Kariapper, et al. (2005). "Sustained hedgehog signaling is required for basal cell carcinoma [roliferation and survival: conditional skin tumorigenesis recapitulates the hair growth cycle." Genes Dev(19): 214-223.

Ichikawa, M., T. Asai, et al. (2004). "AML-1 is required for megakaryocytic maturation and lymphocytic differentiation, but not for maintenance of hematopoietic stem cells in adult hematopoiesis." Nat Med **10**(3): 299-304.

Jackson, S. and J. Bartek (2009). "The DNA-damage response in human biology and disease." Nature **461**(7267): 1071-1078.

Jaks, V., N. Barker, et al. (2008). "Lgr5 marks cycling, yet long-lived, hair follicle stem cells." Nat Genet **40**(11): 1291-1299.

Kemp, C. J. (2005). "Multistep skin cancer in mice as a model to study the evolution of cancer cells." Seminars in Cancer Biology(15): 460-473.

Kopan, R., J. Lee, et al. (2002). "Genetic mosaic analysis indicates that the bulb region of coat hair follicles contains a resident population of several active multipotent epithelial lineage progenitors." Developmental Biology **242**(1): 44-57.

Liu, Y., S. Lyle, et al. (2003). "Keratin 15 promoter targets putative epithelial stem cells in the hair follicle bulge." J Invest Dermatol **121**(5): 953-958.

Lorz, C., C. Segrelles, et al. (2009). "On the origin of epidermal cancers." Curr. Mol. Med.(9): 353-364.

Malanchi, I., H. Peinado, et al. (2008). "Cutaneous cancer stem cell maintenance is dependent on bea-catenin signalling." Nature(452): 650-653.

Massoumi, R., M. Podda, et al. (2006). "Cylindroma as tumor of hair follicle origin." J Invest Dermatol(126): 1182-1184.

McLean, I. W. and P. K. Nakane (1974). "Periodate-lysine-paraformaldehyde fixative. A new fixation for immunoelectron microscopy." J Histochem Cytochem(12): 1077-1083.

Mikhail, F. M., K. K. Sinha, et al. (2006). "Normal and transforming functions of RUNX1: a perspective." J Cell Physiol **207**(3): 582-593.

Missero, C., F. Di Cunto, et al. (2008). "The absence of $p21^{Cip1/WAF1}$ alters keratinocyte growth and differentiation and promotes *ras*-tumor progression." Genes Dev(10): 3065-3075.

Morris, R. J. (2000). "Keratinocyte stem cells: targets for cutaneous carcinogens." J Clin Invest(106): 3-8.

Mukhtar, H. (1995). Skin cancer: mechanisms and human relevance. Florida, CRC Press.

Muller-Rover, S., B. Handjiski, et al. (2001). "A comprehensive guide for the accurate classification of murine hair follicles in distinct hair cycle stages." J Invest Dermatol **117**(1): 3-15.

Nakanishi, M., H. Niida, et al. (2009). "DNA damage responses in skin biology-- implications in tumor prevention and aging acceleration." J Dermatol Sci **56**(2): 76-81.

Navarro, P. (1991). "A role for the E-cadherin cell-cell adhesion molecule during tumor progression of mouse epidermal carcinogenesis." J Cell Biol(115): 517-533.

Oskarsson, T., M. Essers, et al. (2006). "Skin epidermis lacking the *c-myc* gene is resistant to Ras-driven tumorigenesis but can reacquire sensitivity upon additional loss of the $p21^{Cip1}$ gene." Genes Dev(20): 2024-2029.

Osorio, K. M., S. E. Lee, et al. (2008). "Runx1 modulates developmental, but not injury-driven, hair follicle stem cell activation." Development **135**(6): 1059-1068.

Owens, D. M. and F. M. Watt (2003). "Contribution of stem cells and differentiated cells to epidermal tumours." Nat Rev Cancer(3): 444-451.

Park, J., C. J. Strock, et al. (2003). "The ras/raf/MEK/extracellular signal-regulated kinase pathway induced autocrine-paracrine growth inhibition via the leukemia inhibitory factor/JAK/STAT pathway." Mol Cell Biol. **23**(2): 543-554.

Perez-Losada, J. and A. Balmain (2003). "Stem-cell hierarchy in skin cancer." Nature Reviews Cancer **3**(5): 434-443.

Raveh, E., S. Cohen, et al. (2006). "Dynamic expression of Runx1 in skin affects hair structure." Mech Dev **123**(11): 842-850.

Roop, D. R., T. M. Krieg, et al. (1988). "Transcriptional control of high molecular weight keratin gene expression in multistage mouse skin carcinogenesis." Cancer Res(48): 3245-3252.

Schneider, M. R., R. Schmidt-Ullrich, et al. (2009). "The hair follicle as a dynamic miniorgan." Curr Biol **19**(3): R132-142.

Speck, N. A. and D. G. Gilliland (2002). "Core-binding factors in haematopoiesis and leukaemia." Nat Rev Cancer **2**(7): 502-513.

Steelman, L. S., A. S. L., et al. (2008). "Contributions of the Ras/MEF/ERK, PI3K/PTEN/Akt/mTOR and Jak/STAT pathways to leukemia." Leukemia(4): 686-707.

Stenbach, F. (1980). "Adnexal participation in formation of cutaneous tumors following topical application of 9,10-dimethylbenzanthracene." J Cut Pathol(7): 277-294.

Taniuchi, I., M. Osato, et al. (2002). "Differential requirements for Runx proteins in CD4 repression and epigenetic silencing during T lymphocyte development." Cell(111): 621-633.

Taylor, G., M. S. Lehrer, et al. (2000). "Involvement of follicular stem cells in forming not only the follicle but also the epidermis." Cell **102**(4): 451-461.

Topley, G. I., R. Okuyama, et al. (1999). "p21(WAF1/Cip1) functions as a suppressor of malignant skin tumor formation and a determinant of keratinocyte stem-cell potential." Proc Natl Acad Sci U S A **96**(16): 9089-9094.

Trempus, C., R. J. Morris, et al. (2007). "CD34 expression by hair follicle stem cells is required for skin tumor development in mice." Cancer Res **67**(9): 4173-4180.

Trempus, C. S., R. J. Morris, et al. (2003). "Enrichment for living murine keratinocytes from the hair follicle bulge with the cell surface marker CD34." J Invest Dermatol **120**(4): 501-511.

Tumbar, T., G. Guasch, et al. (2004). "Defining the epithelial stem cell niche in skin." Science **303**(5656): 359-363.

Valentino, L. and J. Pierre (2006). "JAK/STAT signal transduction: regulators and implication in hematological malignancies." Biochem Pharmacol **14**(6): 713-721.

Vasioukhin, V., L. Degenstein, et al. (1999). "The magical touch: genome targeting in epidermal stem cells induced by tamoxifen application to mouse skin." Proc Natl Acad Sci U S A **96**(15): 8551-8556.

Venkitaraman, A. (2007). "Chromosomal instability in cancer: causality and interdependence." Cell Cycle **6**(19): 2341-2343.

Vidal, M., L. Salavaggione, et al. (2010). "A role for the epithelial microenvrionment at tumor boundaries: evidence from drosophila and human squamous cell carcinomas." Am J Pathol (Epub ahead of print).

Wang, D. and R. Dubois (2010). "Eicosanoids and cancer." Nat Rev Cancer(3): 181-193.

Ward, J. M., S. Rehm, et al. (1986). "Differential carcinogenic effects of intraperitoneal initiation with 7,12-dimethylbenz(a)anthracene or urethane and topical promotion with 12-O-tetradecanoylphorbol-13-acetate in skin and internal tissues of female SENCAR and BALB/c mice." Environmental Health Perspectives(68): 61-68.

Yu, H., D. Pardoll, et al. (2009). "STATs in cancer inflammation and immunity: a leading role for STAT3." Nat Rev Cancer **9**(11): 798-809.

Zhang, Y., J. Biggs, et al. (2004). "Phorbol ester treatment of K562 cells regulates the transcriptional activity of AML1c through phosphorylation." J. Biol. Chem **279**(51): 53116-53125.

Zhang, Y. V., J. Cheong, et al. (2009). "Distinct Self-Renewal and Differentiation Phases in the Niche of Infrequently Dividing Hair Follicle Stem Cells." Cell Stem Cell.